$$|E^*| = \frac{2}{(A)(DF - K)} \frac{L}{S} \times 10^9 \text{ dyn/cm}^2$$

where A is a constant given by the instrument manual,[12] DF is the value of the dynamic force dial when measuring tan δ, L is the length of sample, S is the cross-sectional area in cm^2, and K is an error constant due to the modulus of electricity and displacement of the stress gauge. Values of Young's modulus E' and the loss modulus E'' were obtained as follows:

$$E' = |E^*| \cos \delta$$

and

$$E'' = |E^*| \sin \delta$$

Acknowledgment. This research was supported by the U.S. Army Research Office, Durham, N.C. Dr. Antonino Recca is indebted to the Italian National Research Council for a fellowship.

References and Notes

(1) J. Garapon, W. H. Beever, and J. K. Stille, *Polym. Prepr., Am. Chem. Soc. Div. Polym. Chem.*, **18**, 138 (1977).
(2) J. Garapon and J. K. Stille, *Macromolecules*, **10**, 627 (1977).
(3) D. F. Lindow and L. Friedman, *J. Am. Chem. Soc.*, **89**, 1271 (1967); L. Friedman and D. F. Lindow, *ibid.*, **90**, 2324 (1968).
(4) L. Friedman and P. W. Rabideau, *J. Org. Chem.*, **33**, 451 (1968).
(5) M. J. S. Dewar and G. J. Gleicher, *Tetrahedron*, **21**, 1817 (1965).
(6) T. C. W. Mark and J. Trotter, *Proc. Chem. Soc., London*, 163 (1961).
(7) R. C. Cass, H. D. Springall, and P. G. Quincey, *J. Chem. Soc.*, 1188 (1955).
(8) L. Cassar, P. E. Eaton, and J. Halpern, *J. Am. Chem. Soc.*, **92**, 3515 (1970).
(9) S. O. Norris and J. K. Stille, *Macromolecules*, **9**, 496 (1976).
(10) W. Wrasidlo, S. O. Norris, J. F. Wolfe, T. Katto, and J. K. Stille, *Macromolecules*, **9**, 512 (1976).
(11) W. Wrasidlo and J. K. Stille, *Macromolecules*, **9**, 505 (1976).
(12) Rheovibron Model DDV-II Instruction Manual 14, August 1969, Tape Measuring Instrument Co., Ltd.

Solid-State and Solution Conformation of *N*-*tert*-Butyloxycarbonyl-L-prolylglycine[1]

E. Benedetti,[2a] V. Pavone,[2a] C. Toniolo,*[2b] G. M. Bonora,[2b] and M. Palumbo[2b]

Istituto Chimico, Università di Napoli, 80134 Napoli, Italy; and Centro di Studi su Biopolimeri, C.N.R., Istituto di Chimica Organica, Università di Padova, 35100 Padova, Italy. *Received June 1, 1977*

ABSTRACT: The occurrence of the oxy analogue in the trans-II 4 → 1 intramolecularly hydrogen-bonded nonhelical peptide conformation, recently proposed for *t*-BOC-L-Pro-Gly-OH in the solid state on the basis of infrared absorption evidence, has been disproved by x-ray diffraction analysis. This type of folding is also absent in polar solvents. However, in solvents of low polarity the presence of this folded form cannot be excluded.

For a full picture of the spatial architecture of peptide molecules the combined application of x-ray diffraction and spectroscopic techniques[3,4] has proved to be highly fruitful. X-ray analysis, while yielding the most exact information on the three-dimensional structure in the crystal state, leaves unanswered questions concerning conformation and conformational equilibria in solution. Such problems may be attacked by a combined use of physicochemical methods so that many important factors influencing peptide conformation (e.g., solvent, temperature, concentration) can be investigated. Obviously, the most reliable and complete information is obtained when solution studies are coupled with x-ray analysis.

We have applied this approach in the present study that represents a part of our continuing investigation of the occurrence, both in the solid state and in solution, of the oxy analogues of the 4 → 1 intramolecularly hydrogen-bonded nonhelical peptide conformations (β turns, C_{10} ring structures).[5] The presence of these folded structures has been recently proposed in the solid state for *t*-BOC-Gly-L-Pro-OH (*t*-BOC, *tert*-butyloxycarbonyl), *t*-BOC-L-Pro-Gly-OH, *t*-BOC-L-Pro-D-Pro-OH, and *t*-BOC-L-Pro-L-Pro-D-Pro-OH on the basis of infrared (IR) absorption evidence.[6] In a previous study from our laboratories[5] we showed by x-ray diffraction that *t*-BOC-Gly-L-Pro-OH does not adopt in the solid state the structure oxy analogous to the β turn (trans-II' type),[6] which however could account, at least in part, for the strong negative Cotton effect near 230 nm observed in the circular dichroism spectra in solvents of low polarity. In this paper we describe the IR absorption and x-ray diffraction results of the second of the *N*-protected peptides listed above, namely *t*-BOC-L-Pro-Gly-OH, in the solid state. Its circular dichroism (CD) and IR absorption properties in solvents of widely different polarity and at different concentrations are also discussed. The conclusions were supported by comparison with the data obtained for a number of derivatives and model compounds.

The structure proposed by Deber[6] for *t*-BOC-L-Pro-Gly-OH (oxy analogue to the *trans*-II β turn) is illustrated in Figure 1.

Experimental Section

Synthesis of Peptides. *t*-BOC-L-Pro-Gly-OMe[7] was synthesized from *t*-BOC-L-Pro-OH and HCl (HCl·H-Gly-OMe) via the dicyclohexylcarbodiimide coupling method:[8,9] mp 67–68 °C, after recrystallization from ethyl acetate–petroleum ether; $[\alpha]^{21}_D$ −63.3° (*c* 0.85; methanol); R_f (TLC; SiO_2; Merck; chloroform–ethanol 9:1) 0.75. *t*-BOC-L-Pro-Gly-OH[10] was prepared by alkaline hydrolysis in an aqueous/dioxane mixture of *t*-BOC-L-Pro-Gly-OMe: mp 171–172 °C, after recrystallization from methanol–ethyl ether; $[\alpha]^{21}_D$ −67.3° (*c* 0.86; methanol); R_f (TLC; SiO_2, Merck; chloroform–ethanol 9:1) 0.15. *t*-BOC-L-Pro-Sar-OMe[11] was synthesized from *t*-BOC-L-Pro-OH and HCl·H-Sar-OMe via the dicyclohexylcarbodiimide method:[8,9] oil, after precipitation with petroleum ether from an ethyl ether solution: $[\alpha]^{21}_D$ −47.2° (*c* 0.94; methanol); R_f (TLC; SiO_2, Merck; chloroform–ethanol 9:1) 0.75. *t*-BOC-L-Pro-Sar-OH[6,12] was prepared by alkaline hydrolysis in an aqueous methanol solvent mixture of *t*-BOC-L-Pro-Sar-OMe: mp 145–146 °C, after recrystallization from ethyl acetate–petroleum ether; $[\alpha]^{21}_D$ −26.5° (*c* 1; dimethylformamide); R_f (TLC; SiO_2, Merck; chlorofrom-ethanol 9:1) 0.10. *t*-BOC-L-Pro-OH and *t*-BOC-L-Pro-OMe were synthesized as described in our previous paper.[13] Ac-Gly-OH was a commercial product (Fluka).

Infrared Absorption. Infrared absorption spectra were recorded using a Beckman Model IR 9 spectrophotometer. For the solid state

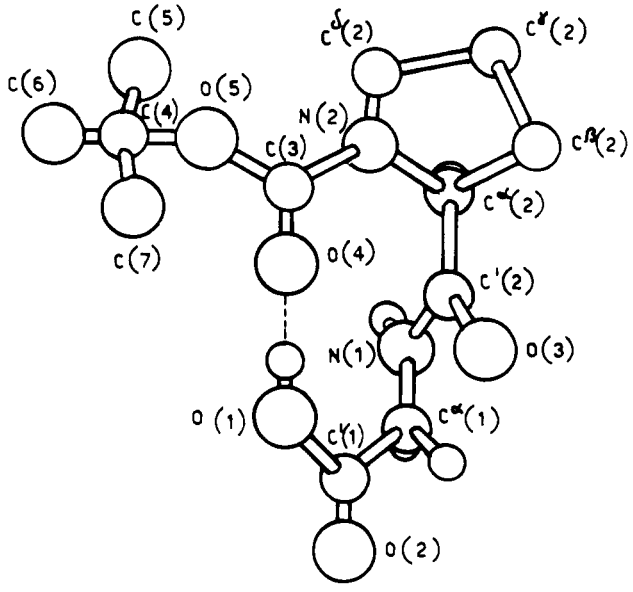

Figure 1. The oxy analogue to the trans-II 4 → 1 intramolecularly hydrogen-bonded nonhelical peptide conformation proposed by Deber[5] for *t*-BOC-L-Pro-Gly-OH in the solid state.

measurements the KBr disk technique was employed. For the solution measurements demountable cells with path lengths ranging from 10 to 0.005 cm and calcium fluoride windows were used. Deuteriochloroform (99.8% *d*) and deuterium oxide (99.9% *d*) were purchased from Merck. The band positions are accurate to ±1 cm^{-1}.

Circular Dichroism. Circular dichroic spectra were recorded using a Cary Model 61 circular dichroism spectrophotometer. The spectra were obtained using cylindrical fused quartz cells of 0.5, 1, and 10 mm path length. Dry prepurified nitrogen was employed to keep the instrument oxygen free during the experiments. A complete baseline was recorded for each measurement using the same cell in which the sample solution had been replaced with pure solvents. Solutions of 10^{-2} to 10^{-3} M peptide were prepared by placing the weighed peptide in a volumetric flask and adding the appropriate solvent. The circular dichroism data represent average values from at least three separate recordings. The calibration was based upon $[\theta]_{290}$ = 7.840 deg cm^2 $dmol^{-1}$ for a purified sample of camphorsulfonic-*10-d* acid (Fluka) in 0.1% aqueous solution. The Lorentz refractive index correction was not applied. The solvents used were double distilled water and spectrograde cyclohexane and chloroform (Merck).

X-Ray Diffraction. Crystals of *t*-BOC-L-Pro-Gly-OH in the form of colorless plates were grown from acetone solutions. Weissenberg photographs showed systematic absences consistent with the orthorhombic space group $P2_12_12_1$. The intensity data collection was carried out on an automatic single-crystal Siemens diffractometer using Ni-filtered Cu Kα radiation (λ 1.5418 Å). A total of 1229 independent reflections were collected and corrected for polarization and Lorentz's factors; 154 of these reflections were not included in the refinement since their values were less than $3\sigma(I)$. The structure was solved by direct methods using the tangent formula in the form programmed by Germain et al.[14] Refinement was achieved by least-squares procedures with anisotropic thermal factors for all atoms except the hydrogen atoms. Their positions were calculated stereochemically and isotropic thermal factors equal to those of the carrier atoms were assigned to each of them. These parameters were kept fixed in the refinement. The weighting scheme proposed by Cruickshank and Pilling[15] was applied; atomic scattering factors were calculated according to Moore.[16] The refinement was ended when the maximum shifts in the atomic coordinates and anisotropic thermal factors were less than 1/5 and 1/3 of the corresponding standard deviations, respectively. The final conventional *R* value was 0.058. A summary of crystal data is given in Table I; the final atomic and thermal parameters together with their estimated standard deviations are given in Table II.

Results and Discussion

Solid-State Conformational Analysis. The IR absorption data of *t*-BOC-L-Pro-Gly-OH, its derivatives, and model compounds in the solid state are listed in Table III. The band

Table I
Crystallographic Data for *t*-BOC-L-Pro-Gly-OH

Mol formula	$C_{12}H_{20}N_2O_5$
Mol wt	272.28
Crystal system	Orthorhombic
Space group	$P2_12_12_1$
Z, molecules/unit cell	4
Cell dimensions,	
a, Å	16.722 ± 0.020
b, Å	6.513 ± 0.018
c, Å	13.162 ± 0.025
V, $Å^3$	1433.53
Density (exptl) by flotation ($CHCl_3$–*n*-hexane), g cm^{-3}	1.25
Density (calcd), g cm^{-3}	1.26
Radiation	Cu Kα (Ni filtered; λ 1.5418 Å)
No. of independent reflections	1075
Temp, °C	21, ambient

positions of the *t*-BOC-L-Pro-Gly-OH match closely those reported by Deber.[6] It is evident that in this particular case the IR absorption properties change only slightly on changing the solvent mixture from which the crystals were obtained. The location of the tertiary urethane (carbamate) carbonyl band (near 1665 cm^{-1}) suggests the participation of this group in hydrogen bonding.[6] In fact, the corresponding free bands in *t*-BOC-L-Pro-OMe and *t*-BOC-L-Pro-Sar-OMe are found at a frequency ≥1700 cm^{-1}, while the strongly hydrogen-bonded band in *t*-BOC-L-Pro-OH[17] appears at 1642 cm^{-1}. However, from the IR absorption data alone it is impossible to discriminate between intramolecular[6] or intermolecular hydrogen-bond formation. In addition, the amide N–H group is also strongly hydrogen bonded, as suggested by its absorption near 3283 cm^{-1}; the N–H stretching absorption of Ac-Gly-OH (Ac, acetyl), that has the N–H group weakly hydrogen bonded in the crystal state,[18–21] falls near 3350 cm^{-1}. Conversely, the position of the carbonyl band of the carboxylic acid of the glycyl residue at about 1775 cm^{-1} indicates that this C=O group is not involved in hydrogen-bond formation[6] (the corresponding absorption of the hydrogen-bonded carbonyl group of the COOH moiety of Ac-Gly-OH[18–21] is found at 1723 cm^{-1}).

The X-ray diffraction analysis of *t*-BOC-L-Pro-Gly-OH allowed us to resolve the ambiguity of the conformational assignment in the solid state made on the basis of its IR absorption properties. The molecular structure is shown in Figure 2; a complete list of bond distances, bond angles, and internal rotation angles are reported in Tables IV–VI.

All parameters shown in Tables IV and V are consistent with known literature data except for the geometry involving the $C^\gamma(2)$ carbon atom, which has an abnormally high component of the thermal parameter along the *c* direction. In fact, the $C^\beta(2)$–$C^\gamma(2)$ and the $C^\gamma(2)$–$C^\delta(2)$ distances are 1.462 and 1.464 Å (Table IV), shorter than the normal carbon–carbon single bond distances, and the $C^\beta(2)$–$C^\gamma(2)$–$C^\delta(2)$ angle is 114.5° (Table V), wider than the usual values.[23,24] The freedom of motion of the $C^\gamma(2)$ carbon atom perpendicular to the mean plane of the remaining atoms of the pyrrolidine ring gives rise to a distribution of conformations for the ring system. The extreme positions of this distribution for the $C^\gamma(2)$ atom (~0.3 Å above and below the mean plane) should correspond to the two possible conformations with γ puckering of the ring.[23–26] The C–O distances in the three types of carbonyl groupings (Table IV) correlate well with the IR absorption data shown in Table III, the highest frequency in the spectrum (about 1775 cm^{-1}) being identified with the carboxylate grouping C′(1)–O(2) which shows the shortest C–O distance (1.182 Å), and the lowest frequencies (about 1665

Table II
Final Atomic Parameters for the C, N, and O Atoms of *t*-BOC-L-Pro-Gly-OH (Esd's Are in Units of the Last Significant Figure)

(A) Positional Parameters

Atom	*x/a*	*y/b*	*z/c*
O(1)	0.4451 (2)	0.5489 (7)	−0.2754 (2)
O(2)	0.5374 (2)	0.5363 (7)	−0.1546 (3)
C′(1)	0.4697 (3)	0.5326 (8)	−0.1802 (4)
$C^{\alpha}(1)$	0.3987 (3)	0.5109 (10)	−0.1088 (4)
N(1)	0.4238 (2)	0.4284 (7)	−0.0119 (3)
C′(2)	0.4514 (3)	0.2358 (9)	−0.0048 (3)
O(3)	0.4484 (2)	0.1116 (6)	−0.0748 (2)
$C^{\alpha}(2)$	0.4930 (2)	0.1842 (8)	0.0947 (3)
$C^{\beta}(2)$	0.5843 (3)	0.1982 (13)	0.0792 (4)
$C^{\gamma}(2)$	0.6135 (3)	−0.0122 (14)	0.0905 (10)
$C^{\delta}(2)$	0.5510 (3)	−0.1645 (10)	0.1103 (4)
N(2)	0.4803 (2)	−0.0313 (7)	0.1234 (3)
C(3)	0.4076 (2)	−0.1127 (8)	0.1417 (3)
O(4)	0.3938 (2)	−0.2958 (5)	0.1522 (3)
O(5)	0.3538 (2)	0.0431 (5)	0.1492 (2)
C(4)	0.2668 (2)	0.0051 (8)	0.1532 (3)
C(5)	0.2453 (3)	−0.0990 (14)	0.2507 (4)
C(6)	0.2410 (3)	−0.1178 (11)	0.0612 (5)
C(7)	0.2351 (3)	0.2237 (10)	0.1492 (5)

(B) Thermal Parameters[a]

Atom	B_{11}	B_{22}	B_{33}	B_{12}	B_{13}	B_{23}
O(1)	5.9 (2)	9.7 (3)	4.6 (1)	1.1 (4)	−0.1 (2)	3.8 (3)
O(2)	4.3 (1)	10.7 (3)	6.1 (2)	−0.5 (3)	0.7 (3)	3.8 (4)
C′(1)	4.8 (2)	5.6 (2)	5.1 (2)	−0.1 (3)	1.0 (3)	2.8 (4)
$C^{\alpha}(1)$	4.5 (2)	9.5 (4)	5.3 (2)	0.4 (5)	1.2 (3)	2.0 (5)
N(1)	5.4 (2)	6.7 (2)	4.2 (1)	−0.4 (3)	1.2 (3)	0.2 (3)
C′(2)	4.2 (1)	7.7 (3)	3.3 (1)	−2.1 (4)	1.8 (3)	−0.3 (3)
O(3)	6.6 (2)	7.7 (2)	3.6 (1)	−0.6 (3)	0.8 (2)	−2.4 (3)
$C^{\alpha}(2)$	4.3 (2)	6.5 (3)	3.4 (2)	−2.0 (4)	0.5 (3)	1.2 (3)
$C^{\beta}(2)$	4.4 (2)	12.2 (5)	6.3 (3)	−3.2 (5)	−1.6 (4)	4.5 (7)
$C^{\gamma}(2)$	4.2 (2)	10.5 (5)	27.6 (1.2)	−2.3 (6)	8.0 (9)	−15.6 (1.4)
$C^{\delta}(2)$	4.0 (2)	10.0 (4)	5.4 (2)	2.8 (5)	1.8 (3)	0.8 (5)
N(2)	3.4 (1)	7.9 (2)	4.4 (1)	1.2 (3)	0.9 (2)	1.0 (3)
C(3)	3.7 (1)	7.1 (3)	3.3 (1)	2.1 (3)	0.8 (3)	−0.6 (4)
O(4)	6.1 (1)	5.0 (2)	5.6 (1)	0.9 (3)	2.5 (3)	0.9 (3)
O(5)	3.6 (1)	5.6 (2)	5.7 (1)	0.0 (2)	1.0 (2)	0.4 (3)
C(4)	3.9 (2)	6.4 (2)	4.2 (2)	0.6 (3)	−0.1 (3)	0.3 (4)
C(5)	4.4 (2)	16.1 (7)	6.4 (3)	2.4 (7)	3.4 (4)	6.7 (8)
C(6)	5.8 (2)	9.9 (4)	7.3 (3)	−0.1 (6)	−3.3 (5)	−3.9 (6)
C(7)	4.8 (2)	7.7 (3)	10.2 (4)	3.4 (5)	.4 (5)	0.0 (6)

[a] $T = \exp[-1/4(B_{11}h^2a^{*2} + B_{22}k^2b^{*2} + B_{33}l^2c^{*2} + 2B_{12}hka^*b^* + 2B_{13}hla^*c^* + 2B_{23}klb^*c^*)]$.

cm^{-1}) with the urethane C(3)–O(4) and amide C′(2)–O(3) groupings, which show the longest distances (1.223 and 1.228 Å, respectively). *t*-BOC-L-Pro-Gly-OH falls, like most amides, outside the curve relating N–H stretching frequencies and N–O distances of crystals containing NH···O hydrogen bonds.[27] The conformation of the *t*-BOC group is such that the C(4)–O(5) bond is cis to C(3)–O(4), as found in all but one urethane *N*-blocked amino acids and peptides,[28] and the methyl groups are staggered with respct to O(4). The conformations about the C(4)–C(methyl) bonds lead to minimal repulsion between the hydrogen atoms. The bond angle O(5)–C(4)–C(7) is 100.7°, notably smaller than tetrahedral. Presumably this pinching is an accommodation to the over-all crowding of the *t*-BOC group, aiding in the relief of the O(4)···C(5) and O(4)···C(6) contacts without worsening the methyl–methyl interactions. Further relief is offered by the opening of the C(4)–O(5)–C(3) angle (122°).

The carboxylic acid group assumes a conformation with respect to the $C^{\alpha}(1)$–N(1) bond which is neither synplanar nor synclinal, since the O(2)–C′(1)–$C^{\alpha}(1)$–N(1) internal rotation angle presents a value of −19° (Table VI).[29] The peptide and urethane groups exhibit significant deviations from planarity; the ω_1 value is 167° (trans configuration) while the ω_2 value is −12° (cis configuration) (Table VI). The mean-square distances of the atoms from the best plane passing through them are 0.068 and 0.055 Å, respectively. The urethane bonds of *t*-BOC-L-Pro-OH[17] and *t*-BOC-(L-Pro)$_4$-OBz[30] were also shown to adopt the cis configuration in the solid state. The internal rotation angles φ, ψ observed for the prolyl residue[23] are not far from the region of the Ramachandran plot corresponding to the conformation of poly(L-proline) I, which also has the imide bonds in the cis configuration.[24,31]

No intramolecular hydrogen bond is present. The molecules are held together in the crystal state by two intermolecular hydrogen bonds (Figure 3): (i) the N(1)–H···O(4) hydrogen bond (2.85 Å) is achieved between the N–H group of the glycyl residue and the oxygen atom of the carbonyl group in the urethane moiety of the molecule translated along the *b* axis; and (ii) the O(1)–H···O(3) strong H bond[32] (2.68 Å) links the O–H group of the carboxylic acid and the oxygen atom of the amide carbonyl group of the prolyl residue of the molecule generated by the screw axis parallel to the *c* direction (the O···O distance is at the limit of the most probable range for O–H···O hydrogen bonds in the crystal state with a carbonyl

Table III
Infrared Absorption Data (cm^{-1}) for t-BOC-L-Pro-Gly-OH, Its Derivatives, and Model Compounds in the Solid State

Compd	N–H stretching	Acid or ester C=O stretching	Urethane C=O stretching	Amide C=O stretching
t-BOC-L-Pro-Gly-OH				
a	3282	1777	1668	1668
b	3284	1777	1667	1667
c		1771	1662	1662
t-BOC-L-Pro-Gly-OMe[b]	3314	1759	1690	1667
t-BOC-L-Pro-Gly-OBz[c]		1755		1660
t-BOC-L-Pro-OH[d]		1742	1642	
t-BOC-L-Pro-OMe[d]		1752	1708	
t-BOC-L-Pro-Sar-OH				
b		1768, 1751	1704, 1693	1612
c		1750 (split)	1688	1604
t-BOC-L-Pro-Sar-OMe[b]		1754	1700	1669
Ac-Gly-OH				
b	3358	1723		~1640 (sh)
e	3346			

[a] This work (crystals obtained from acetone). [b] This work (crystals obtained as indicated in the Experimental Section). [c] Reference 5. [d] Reference 13. [e] Reference 22.

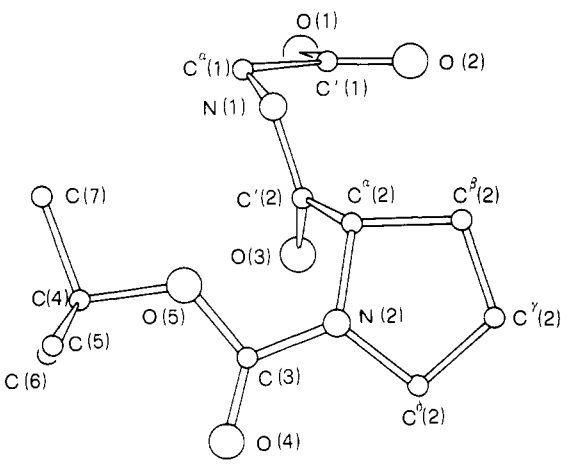

Figure 2. Molecular structure of t-BOC-L-Pro-Gly-OH.

group as hydrogen acceptor).[33] Along the *b* direction the molecules form long rows linked by the N–H···O hydrogen bond; two adjacent rows (in the *bc* plane) form a ribbon of molecules connected by the second hydrogen bond (O–H···O) approximately in the *c* direction. The ribbons pack together by van der Waals interactions in the *a* and *c* directions, so that a certain degree of motion is allowed to both the methyl groups of the t-BOC moiety (in particular the C(5) carbon atom) and the $C^{\gamma}(2)$ carbon atom of the pyrrolidine ring system. Finally, the O(2) atom is not involved in hydrogen bonding.

Thus, the hypothesis of the folding of t-BOC-L-Pro-Gly-OH in the solid state with the formation of the ten-membered ring oxy analogues to the trans-II β turn, put forward on the basis of the IR absorption results, has to be rejected. In fact, the low-frequency value of the urethane carbonyl stretching vi-

Table IV
Bond Distances (Å) for t-BOC-L-Pro-Gly-OH (Esd's Are in Units of the Last Significant Figure)

O(1)–C'(1)	1.323 (6)	$C^{\delta}(2)$–N(2)	1.477 (7)
O(2)–C'(1)	1.182 (5)	N(2)–$C^{\alpha}(2)$	1.469 (7)
C'(1)–$C^{\alpha}(1)$	1.520 (7)	N(2)–C(3)	1.346 (5)
$C^{\alpha}(1)$–N(1)	1.447 (7)	C(3)–O(4)	1.223 (6)
N(1)–C'(2)	1.340 (7)	C(3)–O(5)	1.361 (5)
C'(2)–O(3)	1.228 (6)	O(5)–C(4)	1.475 (5)
C'(2)–$C^{\alpha}(2)$	1.520 (6)	C(4)–C(5)	1.495 (8)
$C^{\alpha}(2)$–$C^{\beta}(2)$	1.543 (6)	C(4)–C(6)	1.515 (8)
$C^{\beta}(2)$–$C^{\gamma}(2)$	1.462 (12)	C(4)–C(7)	1.521 (8)
$C^{\gamma}(2)$–$C^{\delta}(2)$	1.464 (10)		

Table V
Bond Angles (deg) for t-BOC-L-Pro-Gly-OH (Esd's Are in Units of the Last Significant Figures)

O(1)–C'(1)–O(2)	124.6 (2)	$C^{\beta}(2)$–$C^{\gamma}(2)$–$C^{\delta}(2)$	114.5 (3)
O(1)–C'(1)–$C^{\alpha}(1)$	110.4 (2)	$C^{\beta}(2)$–$C^{\alpha}(2)$–N(2)	103.5 (2)
O(2)–C'(1)–$C^{\alpha}(1)$	125.0 (2)	$C^{\gamma}(2)$–$C^{\delta}(2)$–N(2)	101.2 (2)
C'(1)–$C^{\alpha}(1)$–N(1)	110.7 (2)	$C^{\delta}(2)$–N(2)–C(3)	120.8 (2)
$C^{\alpha}(1)$–N(1)–C'(2)	120.6 (3)	N(2)–C(3)–O(4)	125.1 (2)
N(1)–C'(2)–O(3)	123.4 (2)	N(2)–C(3)–O(5)	108.5 (2)
N(1)–C'(2)–$C^{\alpha}(2)$	115.1 (2)	C(3)–O(5)–C(4)	122.0 (2)
C'(2)–$C^{\alpha}(2)$–$C^{\beta}(2)$	109.0 (2)	O(4)–C(3)–O(5)	126.4 (2)
C'(2)–$C^{\alpha}(2)$–N(2)	112.5 (2)	O(5)–C(4)–C(5)	110.1 (2)
O(3)–C'(2)–$C^{\alpha}(2)$	121.3 (2)	O(5)–C(4)–C(6)	110.0 (2)
$C^{\alpha}(2)$–$C^{\beta}(2)$–$C^{\gamma}(2)$	105.2 (3)	O(5)–C(4)–C(7)	100.7 (2)
$C^{\alpha}(2)$–N(2)–$C^{\delta}(2)$	114.5 (2)	C(5)–C(4)–C(6)	112.2 (2)
$C^{\alpha}(2)$–N(2)–C(3)	123.6 (2)	C(5)–C(4)–C(7)	111.8 (2)
		C(6)–C(4)–C(7)	111.6 (2)

Table VI
Internal Rotation Angles (deg) for t-BOC-L-Pro-Gly-OH

O(1)–C'(1)–$C^{\alpha}(1)$–N(1)	162	$C^{\alpha}(2)$–N(2)–C(3)–C(4)	170
O(2)–C'(1)–$C^{\alpha}(1)$–N(1)	−19	$C^{\alpha}(2)$–N(2)–C(3)–O(5)	−12
C'(1)–$C^{\alpha}(1)$–N(1)–C'(2)	−67	$C^{\beta}(2)$–$C^{\gamma}(2)$–$C^{\delta}(2)$–N(2)	−7
$C^{\alpha}(1)$–N(1)–C'(2)–O(3)	−9	$C^{\beta}(2)$–$C^{\alpha}(2)$–N(2)–$C^{\delta}(2)$	−10
$C^{\alpha}(1)$–N(1)–C'(2)–$C^{\alpha}(2)$	167	$C^{\beta}(2)$–$C^{\alpha}(2)$–N(2)–C(3)	182
N(1)–C'(2)–$C^{\alpha}(2)$–$C^{\beta}(2)$	261	$C^{\gamma}(2)$–$C^{\beta}(2)$–$C^{\alpha}(2)$–N(2)	5
N(1)–C'(2)–$C^{\alpha}(2)$–N(2)	147	$C^{\gamma}(2)$–$C^{\delta}(2)$–N(2)–C(3)	179
C'(2)–$C^{\alpha}(2)$–$C^{\beta}(2)$–$C^{\gamma}(2)$	247	$C^{\delta}(2)$–N(2)–C(3)–O(4)	2
C'(2)–$C^{\alpha}(2)$–N(2)–$C^{\delta}(2)$	107	$C^{\delta}(2)$–N(2)–C(3)–O(5)	181
C'(2)–$C^{\alpha}(2)$–N(2)–C(3)	−61	N(2)–C(3)–C(5)–C(4)	170
O(3)–C'(2)–$C^{\alpha}(2)$–$C^{\beta}(2)$	76	O(4)–C(3)–O(5)–C(4)	−11
O(3)–C'(2)–$C^{\alpha}(2)$–N(2)	−37	C(3)–O(5)–C(4)–C(5)	68
$C^{\alpha}(2)$–$C^{\beta}(2)$–$C^{\gamma}(2)$–$C^{\delta}(2)$	1	C(3)–O(5)–C(4)–C(6)	−56
$C^{\alpha}(2)$–N(2)–$C^{\delta}(2)$–$C^{\gamma}(2)$	11	C(3)–O(5)–C(4)–C(7)	186

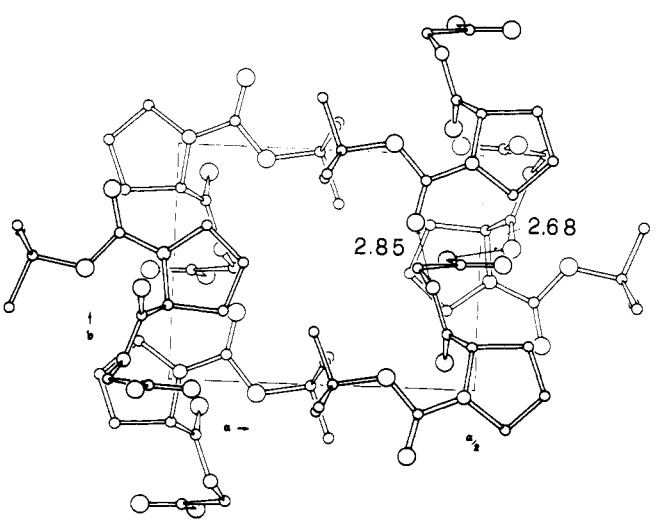

Figure 3. Mode of packing of the t-BOC-L-Pro-Gly-OH molecules projected down the *c* axis. The hydrogen bonds are indicated by arrows.

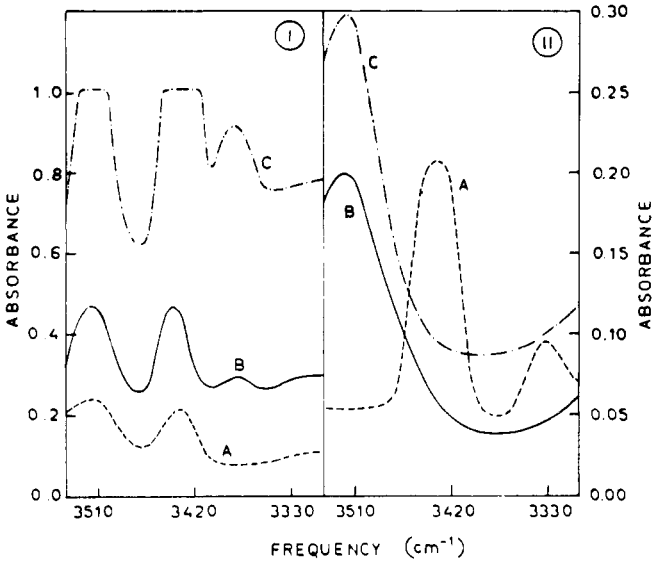

Figure 4. Infrared absorption spectra in the 3540–3300-cm^{-1} region in deuteriochloroform (10-cm cell)(I): *t*-BOC-L-Pro-Gly-OH at 2.9 × 10^{-4} M (A), at 5.80 M (B), and at 1.75 × 10^{-3} M (C); (II) *t*-BOC-L-Pro-Gly-OMe (A), *t*-BOC-L-Pro-OH (B), and *t*-BOC-L-Pro-Sar-OH (C) at ≃3 × 10^{-4} M.

bration is perfectly explainable also in terms of the intermolecular hydrogen bond as found by the present x-ray diffraction analysis. On the other hand, from Figure 2 it is evident that the prerequisite for the formation of the oxy analogues to the β turns in *t*-BOC dipeptides, namely trans urethane –CON< or –CONH– configuration, is not met by *t*-BOC-L-Pro-Gly-OH.

Solution Conformational Analysis. In order to investigate the possible occurrence in solution of the oxy analogues to the β turns in *t*-BOC-L-Pro-Gly-OH we examined its IR absorption and CD properties, along with those of its derivatives and model compounds, in solvents of different polarity and at different concentrations. The interpretation of the results

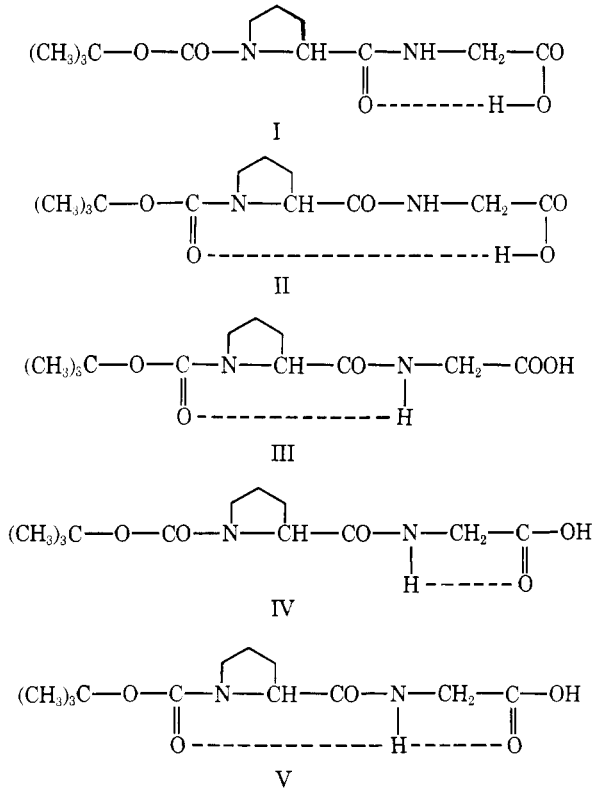

obtained is complicated by the cis–trans isomerism around the prolylurethane bond, already examined for *t*-BOC-L-Pro-Gly-OH and its benzyl ester by ^{13}C nuclear magnetic resonance.[34] In addition, various types of intramolecularly hydrogen-bonded forms (I–V)[31,35] and associated species could account for the spectral properties of *t*-BOC-L-Pro-Gly-OH.

Figure 4I (curve A) shows the IR absorption spectrum of the *N*-protected dipeptide carboxylic acid in deuteriochloroform at high dilution (i.e., in the absence of intermolecular peptide–peptide interactions)[36] in the O–H and N–H stretching region. Two absorptions are clearly visible: we associate the 3518-cm^{-1} band with the "free" (solvated) OH group[37] and the 3435-cm^{-1} band with the "free" (solvated) amide N–H.[31,36,38] These assignments are confirmed by a comparison with the spectra of *t*-BOC-L-Pro-Gly-OMe, *t*-BOC-L-Pro-OH, and *t*-BOC-L-Pro-Sar-OH (Figure 4II). Two other features characterize the curve of *t*-BOC-L-Pro-Gly-OH: an extremely weak band in the region of 3330 cm^{-1} and an increasing absorption with a maximum below 3300 cm^{-1}. A detailed analysis of the region below 3300 cm^{-1} was not carried out because of increasing solvent absorption and possible ambiguity in band assignment.[37] From literature data[24,36,38] and an examination of the spectra of *t*-BOC-L-Pro-Gly-OMe, *t*-BOC-L-Pro-OH, and *t*-BOC-L-Pro-Sar-OH (Figure 4II) the 3330-cm^{-1} band is attributed to the 3 → 1 intramolecularly hydrogen-bonded form ("C_7") (III).[31] The oxy analogue of the 3 → 1 intramolecularly hydrogen-bonded form ("oxy-C_7") (I)[13,31] and the "oxy-C_{10}" form (II) (Figure 1) seem to be absent unless their maxima are located below 3300 cm^{-1} (there is no indication in the literature on where the maxima of these bands are centered). Other types of intramolecularly hydrogen-bonded peptide structures, namely the "C_5" form (IV)[5,24,31,38] and the "C_7C_5" bifurcated hydrogen-bonded form (V),[31,35] are possible. However, the presence of the former is excluded since the corresponding absorption near 3415 cm^{-1} [24,38] is not visible, while that of the latter has not been investigated since its maximum is located below 3300 cm^{-1}.[35] At increasing concentration a new band appears and increases in intensity in the spectrum of *t*-BOC-L-Pro-Gly-OH (but not in that of its methyl ester (not shown)) at 3383 cm^{-1} with a concomitant proportional decrease of the 3518-cm^{-1} band (Figure 4I, curves B and C). The onset of the former absorption should be therefore attributed to associated structures involving O–H···O bonds. This assignment is indirectly corroborated by the observation that peptide structures associated through N–H···O bonds show their hydrogen-bonded N–H band well below 3380 cm^{-1}.[38] However, carboxylic acid dimers cannot be responsible for the 3380-cm^{-1} absorption, their corresponding broad band falling in the region of 3200–2800 cm^{-1}.[39,40]

The IR absorption results in deuteriochloroform and D_2O at high concentration shown in Figure 5, also compared to those reported by Deber[6] and Cung et al.,[38] and to those listed in Table III, indicate that all C=O groups of *t*-BOC-L-Pro-Gly-OH (the carbonyl group of the COOH moiety at 1737 cm^{-1}, the amide carbonyl near 1650 cm^{-1}, and the urethane carbonyl at 1682 cm^{-1}) are hydrogen bonded, although not strongly, in deuteriochloroform; conversely, in D_2O all C=O groups are strongly solvated (the carbonyl absorption of the COOH group is visible at 1728 cm^{-1}, while those of both amide and urethane groups fall in the vicinity of 1660 cm^{-1}).

Hence, it may be reasonably suggested that in deuteriochloroform at high concentration *t*-BOC-L-Pro-Gly-OH is characterized inter alia by an intermolecular hydrogen bond between the OH group and the amide carbonyl, as found in the solid state (see above).

CD is used extensively for conformational assignment of peptide molecules. Recently, Madison and Schellman[41] and

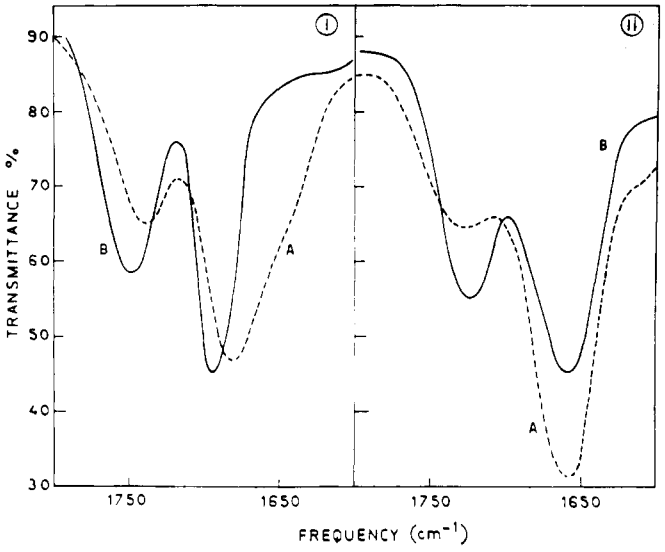

Figure 5. Infrared absorption spectra in the 1800–1600-cm^{-1} region of *t*-BOC-L-Pro-Gly-OH (A) and *t*-BOC-L-Pro-OMe (B) in deuteriochloroform (I) and in D_2O (II) (3.3–4.3 × 10^{-2} M; 0.005-cm cell).

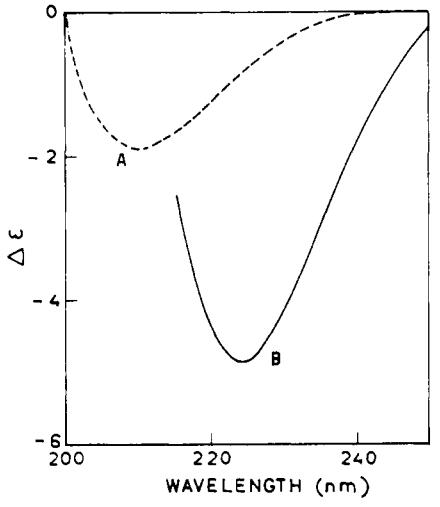

Figure 6. Circular dichroism spectra in the 200–250-nm region of *t*-BOC-L-Pro-Gly-OH in water (A) and in cyclohexane–chloroform 80:20 (v/v) (B) (3.15 × 10^{-3} M).

Cann[42] examined aspects of the CD spectra of *N*-protected L-amino(imino) acids, inculding proline, their esters, and amides in water and in solvents of low polarity. It was found that these compounds exhibit well-developed n → π* amide Cotton effects in the neighborhood of 230 nm in solvents of low polarity as contrasted to scarcely pronounced n → π* amide Cotton effects at about 210 nm in water. It was concluded that these differences are conformationally related and in particular that the strong negative CD maximum near 230 nm arises primarily from intramolecular interaction of the polar hydrogen of the COOH or –CONH– group with the amide (urethane) carbonyl group. The intramolecular hydrogen bond favors one rigid folded conformation of the tertiary amide (in the trans configuration), to which the strong negative CD maximum can be attributed. Space filling models show, however, that either the tertiary amide bond or the intramolecular hydrogen bond but not both can be coplanar. So the rather long-wavelength Cotton effect observed in solvents of low polarity may also involve nonplanar amide bonds.[43] From Figure 6 it is evident that *t*-BOC-L-Pro-Gly-OH in a solvent mixture of low polarity exhibits the strong negative Cotton effect at 225 nm that is absent in aqueous solution.

Table VII
Relationship between Possible Folded Forms and the Presence of the Strong Negative Circular Negative Dichroism Maximum at 225–230 nm in Solvents of Low Polarity

Compd	Possible folded forms			Neg CD max
	"Oxy-C_7"	"Oxy-C_{10}"	"C_7"	
t-BOC-L-Pro-Gly-OH	+	+	+	+[a]
t-BOC-L-Pro-Gly-OMe	–	–	+	+[a]
t-BOC-Gly-L-Pro-OH	+	+	–	+[b]
t-BOC-Gly-L-Pro-OMe	–	–	–	–[b]
t-BOC-L-Pro-OH	+	–	–	+[c]
t-BOC-L-Pro-OMe	–	–	–	–[c]
Ac-L-Pro-OH	+	–	–	+[d,e]
Ac-L-Pro-OMe	–	–	–	–[d]
Ac-L-Pro-NHME	–	–	+	+[d-f]
Ac-L-Pro-NMe_2	–	–	–	–[d]

[a] This work. [b] Reference 4. [c] Reference 13. [d] Reference 41. [e] Reference 43. [f] Reference 42.

However, the three types of intramolecularly hydrogen-bonded folded peptide forms I–III can give rise to such a phenomenon in this compound. To clarify this problem we measured the CD of derivatives and model compounds of *t*-BOC-L-Pro-Gly-OH in the same solvent mixture. The results obtained along with those already published on analogous compounds are summarized in Table VII. Clearly, no definite conformational assignment can be made. In fact, both "oxy-C_7" and "C_7" forms, whose effects on the dichroic properties of *t*-BOC-L-Pro-Gly-OH are not experimentally separable from that of the "oxy-C_{10}" form, can induce the onset of an intense negative CD maximum in the 225–230-nm region. Conversely, from CD measurements alone we cannot exclude the contribution, at least partial, of the "oxy-C_{10}" form to the conformational equilibrium mixture of *t*-BOC-L-Pro-Gly-OH in solvents of low polarity.

In summary, the present x-ray diffraction analysis has demonstrated the absence of the trans-II oxy analogue of the β turn for *t*-BOC-L-Pro-Gly-OH in the solid state, in contrast to the suggestion put forward on the basis of its IR absorption properties.[6] This type of folding is also absent in polar solvents. However, in solvents of low polarity, this intramolecularly hydrogen-bonded folded form could account, at least in part, for the strong negative Cotton effect at 225 nm observed in the CD spectrum. These findings are not surprising, since, in principle, the formation of structures with an intramolecular hydrogen bond in the crystal state is energetically less advantageous than the formation of intermolecularly hydrogen bonded structures.[44]

Clearly, the results of our x-ray diffraction analyses of *t*-BOC-Gly-L-Pro-OH[5] and *t*-BOC-L-Pro-Gly-OH do not rule out the possibility that the frequency shifts observed by Deber[6] in the IR absorption spectra of the other two crystalline prolyl-containing peptides (see above) in the solid state might be indicative of the onset of an oxy analogue to the β turn. The occurrence of this type of folded form in the solid state could possibly be demonstrated also in the oxy analogues to those peptide segments and *N*-protected peptide amides,[24,45–50] the structure of which has already been determined by x-ray diffraction and found to be of the β-turn type. Studies along this line are now in progress in our laboratories, using combined application of IR absorption and x-ray diffraction analysis.

References and Notes

(1) This work is part 42 of the series; for part 41 see M. Palumbo, G. M. Bonora, C. Toniolo, E. Peggion, and E. S. Pysh, "Proceedings Vth American Peptide Symposium", M. Goodman, Ed., San Diego, Calif., in press.
(2) (a) Istituto Chimico, Università di Napoli; (b) Istituto di Chimica Organica, Università di Padova.
(3) (a) Yu. A. Ovchinnikov and V. T. Ivanov, *Tetrahedron*, **31**, 2177 (1975).
(4) C. M. Deber, V. Madison, and E. R. Blout, *Acc. Chem. Res.*, **9**, 106 (1976).
(5) E. Benedetti, M. Palumbo, G. M. Bonora, and C. Toniolo, *Macromolecules*, **9**, 417 (1976).
(6) C. M. Deber, *Macromolecules*, **7**, 47 (1974).
(7) E. Schaich and F. Schneyder, *Hoppe-Seyler's Z. Physiol. Chem.*, **355**, 939 (1974).
(8) J. C. Sheehan and G. P. Hess, *J. Am. Chem. Soc.*, **77**, 1067 (1955).
(9) H. G. Khorana, *Chem. Ind. (London)*, 1087 (1955).
(10) C. M. Deber and E. R. Blout, *Isr. J. Chem.*, **12**, 15 (1974).
(11) A. B. Mauger, R. B. Desai, J. Rittner, and W. J. Rzeszotarski, *J. Chem. Soc., Perkin Trans. 1*, 2146 (1972).
(12) M. Rothe and J. Mazanek, *Justus Liebigs Ann. Chem.*, 439 (1974).
(13) C. Toniolo, M. Palumbo, and E. Benedetti, *Macromolecules*, **9**, 420 (1976).
(14) G. Germain, P. Main, and M. M. Woolfson, *Acta Crystallogr., Sect. A*, **27**, 368 (1971).
(15) K. W. J. Cruickshank and D. E. Pilling, "Computing Methods and the Phase Problem in X-Ray Crystal Analysis", Pergamon Press, Oxford, 1961, p 32.
(16) F. H. Moore, *Acta Crystallogr.*, **16**, 1169 (1963).
(17) E. Benedetti, M. R. Ciajolo, and A. Maistro, *Acta Crystallogr., Sect. B*, **30**, 1783 (1974).
(18) G. B. Carpenter and J. Donohue, *J. Am. Chem. Soc.*, **72**, 2315 (1950).
(19) J. Donohue and R. E. Marsh, *Acta Crystallogr.*, **15**, 941 (1962).
(20) M. F. Mackay and A. Mcl. Mathieson, *Tetrahedron Lett.*, 5069 (1969).
(21) M. F. Mackay, *Cryst. Struct. Commun.*, **4**, 225 (1975).
(22) K. Nakamoto, M. Margoshes, and R. E. Rundle, *J. Am. Chem. Soc.*, **77**, 6480 (1955).
(23) T. Ashida and M. Kakudo, *Bull. Chem. Soc. Jpn.*, **47**, 1129 (1974).
(24) A. Aubry, Ph.D. Thesis, Université de Nancy, 1976.
(25) R. Balasubramanian, A. V. Lakshminarayanan, M. N. Sabesan, G. Tegoni, K. Venkatesan, and G. N. Ramachandran, *Int. J. Protein Res.*, **3**, 25 (1971).
(26) G. N. Ramachandran, A. V. Lakshminarayanan, R. Balasubramanian, and G. Tegoni, *Biochim. Biophys. Acta*, **221**, 165 (1970).
(27) A. Lautié, F. Froment, and A. Novak, *Spectrosc. Lett.*, **9**, 289 (1976).
(28) C. Toniolo and E. Benedetti, unpublished observations.
(29) J. D. Dunitz and P. Strickler, "Structural Chemistry and Molecular Biology", A. Rich and N. Davidson, Ed., W. A. Freeman, San Francisco, Calif., 1968, p 595.
(30) T. Matsuzaki, *Acta Crystallogr., Sect. B.*, **30**, 1029 (1974).
(31) C. Toniolo, *Bioorg. Chem.*, in press, and references therein.
(32) I. D. Brown, *Acta Crystallogr., Sect. A*, **32**, 24 (1976).
(33) J. Mitra and C. Ramakhrisnan, *Int. J. Pept. Protein Res.*, **9**, 27 (1977).
(34) P. E. Young and C. M. Deber, *Biopolymers*, **14**, 1547 (1975).
(35) G. Boussard, M. T. Cung, M. Marroud, and J. Néel, *J. Chim. Phys., (Paris)*, **71**, 1159 (1974).
(36) M. Palumbo, S. Da Rin, G. M. Bonora, and C. Toniolo, *Makromol. Chem.*, **177**, 1477 (1976).
(37) M. St. C. Flett, *J. Chem. Soc.*, 962 (1951).
(38) M. T. Cung, M. Marraud, and J. Néel, *Biopolymers*, **15**, 2081 (1976).
(39) S. Bratoz, D. Hadzi, and N. Sheppard, *Spectrochim. Acta*, **8**, 249 (1956).
(40) R. Blinc, D. Hadzi, and A. Novak, *Z. Elektrochem.*, **64**, 568 (1960).
(41) V. Madison and J. Schellman, *Biopolymers*, **9**, 511 (1970).
(42) J. R. Cann, *Biochemistry*, **11**, 2654 (1972).
(43) H. Faulstich and Th. Wieland, "Peptides 1972", H. Hanson and H. D. Jakubke, Ed., North-Holland Publishing Co., Amsterdam, 1973, p 312.
(44) G. A. Kogan, V. M. Tulchinskii, V. I. Tsetlin, E. N. Shepel, P. V. Kostetskii, and A. I. Miroshnikov, *J. Gen. Chem. USSR (Engl. Transl.)*, **44**, 2022 (1974); A. E. Tonelli: and A. I. Brewster, *J. Am. Chem. Soc.*, **94**, 2852 (1972).
(45) C. Lecomte, A. Aubry, J. Protas, G. Boussard, and M. Marroud, *Acta Crystallogr., Sect. B*, **30**, 1992 (1974).
(46) C. Lecomte, A. Aubry, J. Protas, G. Boussard, and M. Marraud, *Acta Crystallogr., Sect. B*, **30**, 2343 (1974).
(47) A. D. Rudko and B. W. Low, *Acta Crystallogr., Sect. B*, **31**, 713 (1975).
(48) L. L. Reed and P. L. Johnson, *J. Am. Chem. Soc.*, **95**, 7523 (1973).
(49) T. Ueki, T. Ashida, M. Kakudo, Y. Sasada, and Y. Katsube, *Acta Crystallogr., Sect. B*, **25**, 1840 (1969).
(50) T. Ueki, S. Bando, T. Ashida, and M. Kakudo, *Acta Crystallogr., Sect. B*, **27**, 2219 (1971).

Solution Properties of Poly(D-β-hydroxybutyrate). 2. Light Scattering and Viscosity in Trifluoroethanol and Behavior of Highly Expanded Polymer Coils

Y. Miyaki, Y. Einaga,* T. Hirosye, and H. Fujita

Department of Polymer Science, Osaka University, Toyonaka, Osaka, 560 Japan.

Received July 13, 1977

ABSTRACT: This paper aims to investigate solution properties of flexible linear polymers with very large values of the excluded volume parameter z by utilizing a previous finding that trifluoroethanol (TFE) is an unusually good solvent for bacterium-synthesized poly(D-β-hydroxybutyrate) (PHB). A series of PHB fractions with $\overline{M}_w$ up to 10 million are prepared and their TFE solutions at 25 °C are subject to accurate light-scattering and viscosity measurements. After the characteristic parameters for unperturbed chains and the binary cluster integral for segment–segment interactions are estimated by use of Yamakawa's modified Stockmayer–Fixman equation, α_s (linear expansion factor), Ψ (interpenetration function), and α_η (viscosity expansion factor) are calculated as functions of z from observed results. Three findings of principal interest are as follows. (1) As predicted by many theories, α_s^5 becomes asymptotically proportional to z, and the Domb–Barrett semiempirical equation closely describes the observed relation between these two quantities. (2) Ψ is essentially constant (0.22 ± 0.01) for $\alpha_s^3 > 7$. Before approaching this asymptotic behavior, the curve of Ψ vs. α_s^3 shows a slight decline, in contrast to the prediction from the current two-parameter theories. (3) Plots of α_η^3 vs. α_s^3 on a log–log graph are asymptotically represented by a straight line with a slope of 0.90 ± 0.02. This behavior indicates that the Flory viscosity factor Φ decreases steadily as the polymer coils undergo increasing expansion by volume exclusion.

In Part 1[1] of this series we concluded from a variety of experimental observations that the molecular chain of a bacterium-produced poly(D-β-hydroxybutyrate) (PHB) in such solvents as trifluoroethanol (TFE), ethylene dichloride (EDC), and chloroform assumes randomly coiled conformation and undergoes unusually large excluded volume effects. In fact, the observed molecular weight dependence of $\langle S^2 \rangle$ (mean-square radius of gyration), A_2 (second virial coefficient), and $[\eta]$ (intrinsic viscosity) for the polymer in TFE approached one which may be expected from the current theories of dilute polymer solutions for very large values of β, the binary cluster integral for segment–segment interaction. It occurred to us that such features of the system PHB–TFE could be utilized for exploring one of the yet unsettled problems in polymer